Research in Nondestructive Evaluation
Publication details, including instructions for authors and subscription information:
http://www.informaworld.com/smpp/title~content=t713723477

Reconstruction of Crack Clusters in the Rectangular Domain by Ultrasonic Waves

M. Brigante[a]; M. A. Sumbatyan[b]
[a] Department of Structural Engineering, University of Naples - Federico II, Naples, Italy [b] Faculty of Mathematics, Mechanics, and Computer Science, Southern Federal University, Rostov-on-Don, Russia

Online publication date: 13 October 2010

To cite this Article Brigante, M. and Sumbatyan, M. A.(2010) 'Reconstruction of Crack Clusters in the Rectangular Domain by Ultrasonic Waves', Research in Nondestructive Evaluation, 21: 4, 193 — 212
To link to this Article: DOI: 10.1080/09349847.2010.490004
URL: http://dx.doi.org/10.1080/09349847.2010.490004

Research in Nondestructive Evaluation, 21: 193–212, 2010

ISSN: 0934-9847 print/1432-2110 online
DOI: 10.1080/09349847.2010.490004

Taylor & Francis
Taylor & Francis Group

RECONSTRUCTION OF CRACK CLUSTERS IN THE RECTANGULAR DOMAIN BY ULTRASONIC WAVES

M. Brigante[1] and M. A. Sumbatyan[2]

[1]Department of Structural Engineering, University of Naples – Federico II, Naples, Italy
[2]Faculty of Mathematics, Mechanics, and Computer Science, Southern Federal University, Rostov-on-Don, Russia

In the present article we study the reconstruction problem for clusters of linear cracks inside a rectangular domain. The parameters to be reconstructed are the number of cracks and the size and slope of each defect. The scanning is performed by a single ultrasonic transducer placed at a certain boundary point. The input data, used for the reconstruction algorithm, is taken as measured oscillation amplitudes over an array of chosen boundary points. The proposed numerical algorithm is tested on some examples with multiple clusters of cracks whose position and geometry are known a priori.

Keywords: BEM, crack clusters, global random search, optimization, reconstruction, rectangular domain

1. INTRODUCTION

In many engineering applications there arise the problems of identification of unknown objects located in some domains, the so-called image recognition. Various methods are used to study such problems. In the non-destructive testing (NDT) of materials, the acoustic and electromagnetic methods are based on wave properties of damaged materials, and their difference from analogous properties of perfect (undamaged) bodies. The problem of identification of the underground near-surface texture as well as defects arising in masonry architectural structures is being successfully studied by using both acoustic and electromagnetic waves [1–3]. In particular, ultrasonic techniques [4] demonstrate high efficiency in defect identification. Other acoustic methods are connected with measurements of dynamic wave fields over some parts of the sample's boundary, under condition that the latter is loaded by a certain oscillating force. Some theoretical works prove that the shape of the boundary can uniquely determine the geometry of the internal defects [5–7]. A contiguous method is founded upon measurements of the natural frequencies of the sample. In fact, the change of the geometry of internal defects influences significantly the measurable set of

Address correspondence to M. A. Sumbatyan, Faculty of Mathematics, Mechanics, and Computer Science, Southern Federal University, Milchakova Street 8a, 344090 Rostov-on-Don, Russia. E-mail: sumbat@math.rsu.ru

natural frequencies. This permits the reconstruction on the basis of alternative ideas.

It should be noted that from the mathematical point of view the reconstruction problem under consideration is a typical inverse problem. During the latest decades, the theory of inverse problems has been developed very intensively [8–10]. This theory is connected with ill-posed problems [11], which generate instability when one applies standard direct numerical methods to construct the solution.

The main goal of the present work is to develop an efficient algorithm to solve the reconstruction problem in the case when a set of linear cracks are located in the rectangular specimen. The investigation is performed under the assumption of scalar ultrasonic wave propagation [4]. This means that in the case of solid specimen, where both longitudinal and transverse types of waves may propagate through the domain, we assume that one of them plays predominant role, so that the second one can be neglected. We first develop an appropriate form of the Green's function in the rectangular domain. Then by a standard approach known in the classical potential theory, we reduce the wave problem in the damaged rectangle to a Boundary Integral Equation (BIE). The reconstruction problem is formulated as follows. Assume the rectangle containing a set of internal cracks is loaded by a harmonic pressure source at a certain point of its outer boundary. If one can measure the amplitude of harmonic oscillations over the boundary line, then one can try to restore the full information about the number and the geometry of all defects. We do not pay much attention to such fundamental questions as existence and uniqueness. Instead we develop an efficient algorithm for practical reconstruction.

2. FORMULATION OF THE PROBLEM

Let a rectangular domain $(0, a) \times (0, b)$ represent a specimen that admits propagation of acoustic waves, in frames of two-dimensional problem. A cluster of N_c linear cracks may appear in the specimen, and the problem is to reconstruct their number, position, and geometry, by using ultrasonic scanning. Generally, each crack may have its own length and slope. The scanning is performed by a single surface harmonic source s_0 with the circular frequency ω. In order to be more specific, let us assume that the source is applied at the point $(x_0, 0)$, so that $p = s_0\delta(x - x_0)$ over the lower face of the rectangle, where δ is Dirac's delta-function. All other faces of the specimen are free of load, hence the boundary condition is trivial there: $p = 0$ over remaining part of the boundary. The dependence of all physical quantities upon time is taken in the form $e^{-i\omega t}$.

Let us assume a cluster of linear cracks to be located in the rectangular domain (see Fig. 1), and l_n, $(n = 1, \ldots, N_c)$ denotes the surface of n th

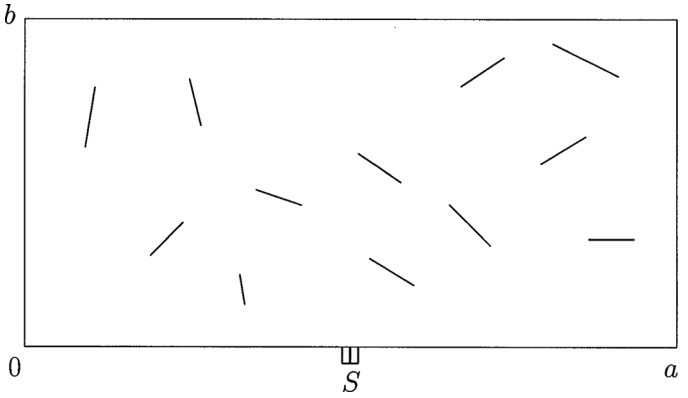

FIGURE 1. A cluster of cracks in the rectangular sample (*S* designates the point acoustic source).

crack. Then the acoustic pressure $p(x, y)$ in the damaged specimen satisfies the Helmholtz equation [4]

$$\frac{\partial^2 p}{\partial x^2} + \frac{\partial^2 p}{\partial y^2} + k^2 p = 0, \qquad k = \frac{\omega}{c} \tag{2.1}$$

where wave number k is associated with that type of wave, among two ones, which play the dominant role.

The boundary conditions to Eq. (2.1) are described above. Let us denote the full set of cracks by l: $l = \bigcup_{n=1}^{N_c} l_n$, and the full outer boundary line (which consists of four straight-line segments) by L. If the internal faces of defects are free of load, then the boundary condition over l and on the outer boundary contour L are

$$p(x, y)|_l = 0, \qquad p(x, y)|_L = s_0 \delta(x - x_0)\delta(y). \tag{2.2}$$

Taking into account that the problem in concern is linear, it is possible to represent the full solution to the direct problem as a superposition of the function $p_0(x, y)$ corresponding to outer load (2.2) applied to the perfectly continuous (i.e., without any flaw) rectangle, and the one $p_1(x, y)$ corresponding to the problem with trivial boundary conditions over the outer contour L, with the cracks l subjected to a certain pressure

$$p(x, y) = p_0(x, y) + p_1(x, y), \qquad p_0(x, y)|_L = s_0 \delta(x - x_0)\delta(y). \tag{2.3}$$

This results in the following boundary value problem for function p_1:

$$\frac{\partial^2 p_1}{\partial x^2} + \frac{\partial^2 p_1}{\partial y^2} + k^2 p_1 = 0; \quad p_1(x, y)|_l = -p_0(x, y)|_l; \quad p_1(x, y)|_L = 0. \tag{2.4}$$

3. A SPECIAL FORM OF GREEN'S FUNCTION

Since the applied technique is based upon the BIE method [12], the key role for further discussion is played by Green's function. There are some classical approaches known in literature to construct Green's function in the rectangular domains [13,14], but final representations are not so simple to be used directly. In order to attain a more simple form of respective expressions, in the present section we develop a special appropriate form of Green's function.

Let us construct the Green's function for the considered rectangular domain, i.e., function $\Phi(\xi, \eta, x, y)$ satisfying the inhomogeneous Helmholtz equation with homogeneous boundary condition

$$\frac{\partial^2 \Phi}{\partial \xi^2} + \frac{\partial^2 \Phi}{\partial \eta^2} + k^2 \Phi = -\,\delta(\xi - x)\,\delta(\eta - y), \qquad \Phi|_{(\xi,\eta)\in L} = 0. \tag{3.1}$$

It should be noted that point (x, y) in (3.1) is an arbitrary fixed point inside the rectangle.

Let us represent the solution to Eq. (3.1) in the form

$$\Phi(\xi, \eta) = \sum_{m=1}^{\infty} \sin\left(\frac{\pi m \xi}{a}\right) \Phi_m^*(\eta). \tag{3.2}$$

Obviously, this representation automatically satisfies the trivial boundary conditions on the left ($\xi = 0$) and right ($\xi = a$) boundary sides of the rectangle.

Substitution of (3.2) into (3.1), after taking a scalar product of the arising relation with functions $\sin(\pi \bar{m} \xi / a)$ over the interval $0 \le x \le a$, due to natural orthogonality of trigonometric functions, results in the following ordinary differential equation regarding function $\Phi_m^*(\eta)$:

$$\Phi^{*\prime\prime} - q_m^2\, \Phi^* = -\,\frac{2}{a} \sin\left(\frac{\pi m x}{a}\right) \delta(\eta - y), \quad q_m = \sqrt{\left(\frac{\pi m}{a}\right)^2 - k^2}, \tag{3.3}$$

where the subscript m in designation of function $\Phi_m^*(\eta)$ is omitted for the sake of brevity.

The solution to this inhomogeneous equation can be obtained as a general solution of the respective homogeneous equation,

$$\Phi_h^* = C_1 \sinh(q_m \eta) + C_2 \sinh[q_m(\eta - b)], \tag{3.4}$$

plus a particular solution to the full inhomogeneous equation. Since the latter may not satisfy the boundary conditions over the horizontal boundary sides,

$y=0,\ b$, this can be constructed by applying the Fourier transform with respect to η over the infinite axis

$$\tilde{\Phi}_p^*(\beta)=\int_{-\infty}^{\infty}\Phi_p^*(\eta)e^{i\beta\eta}\,d\eta,\quad \Phi_p^*(\eta)=\frac{1}{2\pi}\int_{-\infty}^{\infty}\tilde{\Phi}_p^*(\beta)e^{-i\beta\eta}\,d\beta. \tag{3.5}$$

Application of the Fourier transform to Eq. (3.3) reduces the latter to the following simple algebraic equation:

$$\begin{aligned}-\beta^2\tilde{\Phi}_p^*(\beta)-q_m^2\,\tilde{\Phi}_p^*(\beta)&=-\frac{2}{a}\sin\Big(\frac{\pi mx}{a}\Big)e^{i\beta y}\\ \Rightarrow\tilde{\Phi}_p^*(\beta)&=\frac{2}{a}\sin\Big(\frac{\pi mx}{a}\Big)\frac{e^{i\beta y}}{\beta^2+q_m^2},\end{aligned} \tag{3.6}$$

whose Fourier inversion over β is

$$\Phi_p^*(\eta)=\frac{\sin(\pi mx/a)}{a\ q_m}\ e^{-q_m|y-\eta|}. \tag{3.7}$$

Therefore, the full solution to Eq. (3.3) is

$$\Phi^*=C_1\sinh(q_m\eta)+C_2\sinh[q_m(\eta-b)]+\frac{\sin(\pi mx/a)}{a\ q_m}\ e^{-q_m|y-\eta|}. \tag{3.8}$$

The unknown constants should be determined from the two boundary conditions, which are $\Phi^*(\eta=0,b)=0$, that defines these constants in the following form

$$C_1=-\frac{\sin(\pi mx/a)}{a\ q_m\sinh(q_mb)}\ e^{-q_m(b-y)},\quad C_2=\frac{\sin(\pi mx/a)}{a\ q_m\sinh(q_mb)}\ e^{-q_my}. \tag{3.9}$$

Now, collecting together Eqs. (3.2), (3.8), (3.9), one arrives at the representation

$$\begin{aligned}\Phi(\xi,\eta,x,y)=\sum_{m=1}^{\infty}\frac{\sin(\pi m\xi/a)\sin(\pi mx/a)}{a\ q_m\sinh(q_mb)}\times\{&\sinh[q_m(\eta-b)]e^{-q_my}\\ &-\sinh(q_m\eta)e^{-q_m(b-y)}+\sinh(q_mb)e^{-q_m|\eta-y|}\Big\}.\end{aligned} \tag{3.10}$$

It can be shown, by applying expansion of trigonometric and hyperbolic functions with difference and sum of two arguments, that formula (3.10) can also be rewritten in the following equivalent form:

$$\Phi(\xi,\eta,x,y)=\frac{2}{a}\sum_{m=1}^{\infty}\frac{\sin(\pi m\xi/a)\sin(\pi mx/a)}{q_m\sinh(q_mb)}\times\left\{\begin{array}{ll}\sinh[q_m(b-\eta)]\sinh(q_my), & \eta\geq y,\\ \sinh[q_m(b-y)]\sinh(q_m\eta), & \eta<y.\end{array}\right\}. \tag{3.11}$$

One more equivalent representation of Green's function can be extracted from (3.11), after some routine transformations:

$$\Phi(\xi,\eta,x,y)=\frac{1}{a}\sum_{m=1}^{\infty}\frac{\sin(\pi m\xi/a)\sin(\pi mx/a)}{q_m\sinh(q_mb)}\times\{\cosh[q_m(b-|\eta-y|)]-\cosh[q_m(b-\eta-y)]\}, \tag{3.12}$$

which is also equivalent to the following form containing for each m a sum of four more elementary terms:

$$\begin{aligned}\Phi(\xi,\eta,x,y)=\frac{1}{2a}\sum_{m=1}^{\infty}\frac{1}{q_m\sinh(q_mb)}\times\Bigg\{&\cos\left(\pi m\frac{\xi-x}{a}\right)\cosh[q_m(b-|\eta-y|)]\\&-\cos\left(\pi m\frac{\xi+x}{a}\right)\cosh[q_m(b-|\eta-y|)]\\&+\cos\left(\pi m\frac{\xi+x}{a}\right)\cosh[q_m(b-\eta-y)]\\&-\cos\left(\pi m\frac{\xi-x}{a}\right)\cosh[q_m(b-\eta-y)]\Bigg\}.\end{aligned} \tag{3.13}$$

It should be noted that if the points (ξ, η) and (x, y) both lie inside the rectangle, then for all four terms in (3.13) the second argument $\eta\pm y$ is such that $|\eta\pm y|<2b$, so $-b<b-|\eta\pm y|<b$. This predetermines the series (3.13) to converge not slower than a geometric progression. It is also easily seen that the constructed Green's function (3.11) satisfies the required trivial Dirichlet boundary conditions indeed.

4. DERIVATION OF THE BASIC BIE

The constructed Green's function permits derivation of the principal unknown function $p_1(x, y)$ inside the rectangle as an integral over the cracks faces, contour l, with the use of standard methods of potential theory [12]

$$p_1(x,y)=\left(\int_{\Gamma}+\int_{L}\right)\left(p_1\frac{\partial\Phi}{\partial n}-\Phi\frac{\partial p_1}{\partial n}\right)dl, \tag{4.1}$$

where both the outer unit normal vector $\mathbf{n}(\xi, \eta)$ and the elementary arc of length $dl(\xi, \eta)$ are connected with the point (ξ, η), not (x, y). Besides, we imply that contour $\Gamma = \bigcup_{n=1}^{N_c} \Gamma_n$ and each elementary boundary curve Γ_n represents itself a smooth closed contour surrounding the crack l_n ''face to face,'' since the basic integral representation (4.1) is valid for closed smooth contours only [12].

Now it becomes clear why so specifically constructed Green's function is very important in the problem at hand. In fact, both Φ and p_1 functions vanish over the outer boundary of the domain, due to boundary conditions (2.4) and (3.1). Therefore, the second integral over contour L is trivial, and there remains only the integral over Γ in representation (4.1).

Let us prove that

$$\int_{\Gamma} \left(p_0 \frac{\partial \Phi}{\partial n} - \Phi \frac{\partial p_0}{\partial n} \right) dl = 0. \tag{4.2}$$

The proof is founded upon the fact that both functions $p_0(\xi, \eta)$ and $\Phi(\xi, \eta, x, y)$ are regular inside the rectangle. Hence, they possess the same value on the opposite sides of the crack. Besides, since the direction of normal $\mathbf{n}$ is opposite on the opposite cracks' faces, the normal derivatives of these functions have the same values with opposite sign. Therefore, the contributions of the quantities along opposite cracks' faces in (4.2) cancel to each other.

Now, by summation of (4.1) and (4.2), one can express $p_1(x, y)$ in terms of boundary values of the full pressure $p(x, y)$ and its normal derivative

$$p_1(x, y) = \int_{\Gamma} \left(p \frac{\partial \Phi}{\partial n} - \Phi \frac{\partial p}{\partial n} \right) dl = - \int_{\Gamma} \frac{\partial p}{\partial n} \Phi dl, \tag{4.3}$$

due to boundary condition (2.2).

Now, by bringing nearer surrounding smooth contour Γ_n close to the faces of the current crack, one can see that function Φ possesses again equal values at opposite points of the two crack faces. Then, by introducing the new unknown function g as a sum of normal derivative of pressure at two opposite sides of the crack: $g(\xi, \eta) = (\partial p/\partial n)^{(1)} + (\partial p/\partial n)^{(2)}$, one can write out representation (4.3) with the integration contour coinciding with the true full set l of cracks' segments

$$p_1(x, y) = - \int_{l} g(\xi, \eta) \Phi(\xi, \eta, x, y) dl. \tag{4.4}$$

By using well-known boundary value of the potential of single layer [12], if any $(X, Y) \in l$, then

$$\lim_{(x,y) \to (X,Y)} \int_{l} g(\xi, \eta) \Phi(\xi, \eta, x, y) dl = \int_{l} g(\xi, \eta) \Phi(\xi, \eta, X, Y) dl. \tag{4.5}$$

With such a limit $(x,\ y) \to (X,\ Y) \in L$, Eq. (4.4) allows one to formulate the basic BIE in the form

$$\int_l g(\xi,\eta)\Phi(\xi,\eta,X,Y)dl = p_0(X,Y), \quad (X,Y) \in l, \tag{4.6}$$

since $p_1 = p - p_0$ and due to boundary condition (2.2). One thus can see that if the geometry of the full set of cracks l is known a priori, then the problem can be reduced to a system of Fredholm integral equations of the first kind holding over cracks' segments. It should be noted that kernels of these integral equations coincide with Green's function, so they possess a logarithmic singularity when $(\xi,\ \eta) \to (X,\ Y)$ [12].

In order to complete formulation of the basic BIE (4.6), let us construct its right-hand side, function $p_0(X,\ Y)$. This can be performed by analogy to the method applied to derive respective representation for function Φ. Namely, one may seek solution to the Helmholtz equation with boundary condition (2.3) again as a Fourier series analogous to Eq. (3.2)

$$p_0(x,y) = \sum_{m=1}^{\infty} \sin\left(\frac{\pi m x}{a}\right)\varphi_m(y), \quad \Rightarrow \quad \varphi_m'' - q_m^2\ \varphi_m = 0,$$
$$\Rightarrow \quad \varphi_m(y) = B_m \sinh(q_m y) + D_m \sinh[q_m(y-b)]. \tag{4.7}$$

Now, due to orthogonality of the trigonometric functions, boundary condition $p_0(x,\ b) = 0$ implies $B_m = 0$. Then the remaining boundary condition, at $y = b$, is reduced to the following equality:

$$-\sum_{m=1}^{\infty} D_m \sinh(q_m b)\sin\left(\frac{\pi m x}{a}\right) = s_0\delta(x - x_0), \quad D_m = -\frac{2s_0}{a}\frac{\sin(\pi m x_0/a)}{\sinh(q_m b)}. \tag{4.8}$$

The substitution of (4.8) into (4.7) results in the following expression:

$$p_0(x,y) = \frac{2s_0}{a}\sum_{m=1}^{\infty} \sin\left(\frac{\pi m x}{a}\right)\sin\left(\frac{\pi m x_0}{a}\right)\frac{\sinh[q_m(b-y)]}{\sinh(q_m b)}. \tag{4.9}$$

So long as the principal system of BIE (4.6) with the kernel taken in one of forms (3.10)–(3.13) and the right hand-side in the form (4.9) is solved, the acoustic pressure at arbitrary internal point $(x,\ y)$ of the rectangular domain can be found from Eq. (4.4).

5. MATHEMATICAL ASPECTS OF THE RECONSTRUCTION PROBLEM

As indicated in the final part of the previous section, as soon as integral Eq. (4.6) is solved, i.e., function $g(\xi, \eta)$ is defined, the acoustic wave field at any point inside the rectangle can be calculated from Eq. (4.4). In particular, one can place ultrasonic probes over some parts of the boundary surface of the specimen, in order to measure the amplitude of oscillations at a current boundary point. Assume this amplitude to be determined by the normal component of the velocity. By neglecting a certain inessential factor, this velocity is defined by the normal derivative of the acoustic pressure $(\partial p/\partial n)|_L$. Since one can predict the dynamic behavior of the free surface, under the same harmonic loading, in the case of no crack inside the body, hence one can easily observe the contribution given by the presence of the flaws, i.e., normal derivative of p_1 at the chosen boundary points of contour L. The latter can be calculated on the basis of Eq. (4.6) in the following way:

$$F_0(x,y) = \frac{\partial p_1(x,y)}{\partial n} = -\int_l g(\xi,\eta)\frac{\partial \Phi(\xi,\eta,x,y)}{\partial n_{xy}}\,dl, \qquad (x,y)\in L, \quad (5.1)$$

and the normal is applied this time at the point (x, y), not (ξ, η).

Let us write out explicitly the normal derivative of Green's function. If $\mathbf{n} = \{n_x, n_y\}$ is the outer unit normal vector to the boundary contour L of the defect, then it follows from Eq. (3.11) that

$$\begin{aligned}\frac{\partial \Phi}{\partial n_{xy}} = \frac{\partial \Phi}{\partial x}n_x + \frac{\partial \Phi}{\partial y}n_y = \frac{1}{a}\sum_{m=1}^{\infty}\frac{\sin(\pi m\xi/a)}{\sinh(q_m b)} \\ \times\left\langle \frac{\pi m}{a\,q_m}\cos\left(\frac{\pi m x}{a}\right)\{\cosh[q_m(b-|\eta-y|)] \right. \\ -\cosh[q_m(b-\eta-y)]\}n_x \\ +\sin\left(\frac{\pi m x}{a}\right)\{\sinh[q_m(b-|\eta-y|)]\mathrm{sign}(\eta-y) \\ \left. +\sinh[q_m(b-\eta-y)]\}n_y\right\rangle.\end{aligned} \quad (5.2)$$

The reconstruction problem is formulated as follows. Let us assume that unknown number N_c, $(1 \le N_c \le N^*)$ of cracks, each with unknown position and canting angle are located somewhere inside the rectangle. Let us put a point acoustic source s_0 at a certain boundary point $(x_0, 0)$ and measure the amplitude of velocity oscillations over the outer boundary of the domain. Then, by knowing this measured oscillation, it is required to predict the number of cracks, their position, and, their geometry. It is obvious that mathematically the problem is to determine the listed quantities from the known

function $F_0(x, y)$ (5.1). Since another unknown function $g(\xi, \eta)|_{(\xi, \eta)\in l}$ is involved in all mathematical formulas, this means that mathematically one needs to solve the system of two integral Eqs. (4.6) and (5.1), which are nonlinear regarding equation of contour l. It should also be noted that we restrict the possible maximum number of cracks by a certain quantity N^*.

Generally, the problem on cracks reconstruction was studied intensively during some decades past, because of its importance in engineering applications. This is connected with the fundamental theory of inverse problems (some interesting theoretical results with further references can be found in [5–10]). The mathematical results of this sort concern uniqueness of the solution, some others develop explicit-form analytical solutions. Unfortunately, there are too few published papers devoted to efficient algorithms of the reconstruction. In particular, there are no published works on concrete reconstruction algorithms in the case of multiple cracks located in bounded domains.

In the next section we give the details of a reconstruction algorithm, which in the case of arrays of cracks is founded on the system of BIE developed in the previous sections. The reconstruction will be reduced to an optimization problem for a certain strongly nonlinear objective functional. A special stochastic numerical technique will be applied to solve this optimization problem.

It should be noted that for the case of a single volumetric flaw in the half-space, in frames of dynamic elasticity theory, an interesting method based on BIE theory, was proposed in [15].

6. SOME DETAILS OF NUMERICAL ALGORITHM

When solving the basic system of BIE over the cluster of cracks we apply the co-location technique. If all contours l_n are known, then one can arrange a dense set of nodes (X_i, Y_i), $i = 1, \ldots, J_n$, which subdivides the contour to J_n small intervals of equal length h_n. In practice, the length of the step depends upon the wave length connected with the frequency of oscillations, as well as upon the length of the n th crack. In any way, one should take at least ten nodes along the wave length. In order to be more specific, let us take into account the well-known fact in the ultrasonic detection: it is not realistic to detect cracks whose size is less than the wave length λ. We thus assume, when developing our algorithm, that the cracks lengths all are greater than the wave length (equality of the two quantities is admitted too). Starting from this assumption, we accept all elementary intervals over all cracks to be of the same length $h = h_n = \lambda/10$. This guarantees that in the worst case, when the length of the crack is equal to λ, the minimum number of grid nodes over the crack is 10. For real defects, like in masonry structures, this number is significantly greater than 10. Obviously, the total number of nodes is $J = \sum_{n=1}^{N_c} J_n$, where again N_c is the number of cracks, and the full length of cracks in the cluster is hJ.

As follows from the general theory (see, for example, [12]), if $h \to 0$, then the approximate numerical solution to Eq. (4.6) can be obtained by approximating the integrals by some quadrature formulas. The simplest way is to approximate the full integrand by a piecewise constant function. The only problem here is that when solving Fredholm equations of the first kind, the qualitative properties of the kernels must be taken into account in their true from. In our problem, the kernels possess a logarithmic singularity as $(\xi, \eta) \to (X, Y)$. In order to use correctly this singularity in the integration, it should be extracted in its explicit form.

The kernel of the developed BIE (4.6) coincides with Green's function. Let us start from the representation of Green's function taken in the form (3.13). It can be easily seen that if both points (ξ, η) and (x, y) lie somewhere inside the rectangle, then the principal behavior of the Green's function is defined by the first term in the brackets, among all other four terms presented in (3.13). Really, the third and the fourth terms in the brackets generate exponentially convergent series as $(\xi, \eta) \to (x, y)$, because in the case $0 < y < b \sim -b < b - 2y < b$ the ratio $\cosh[q_m(b-2y]/\sinh(q_m b)$ provides exponential decay with parameter m increasing. The behavior of the series generated by the second term in the brackets is predetermined by the properties with large m, where the series is degenerated to the following tabulated form [16]:

$$\frac{1}{2\pi}\sum_{m=1}^{\infty}\frac{1}{m}\cos\left(\frac{2\pi m x}{a}\right) = -\frac{1}{2\pi}\ln\left|2\sin\left(\frac{\pi x}{a}\right)\right|, \tag{6.1}$$

the value which remains finite if $0 < x < a$.

The first term in (3.13) is again defined qualitatively by its behavior for large m generating, when $(\xi, \eta) \to (x, y)$, the following series [16]:

$$\begin{aligned}
\Phi(\xi,\eta,x,y) &\approx \frac{1}{2\pi}\sum_{m=1}^{\infty}\frac{\cos[\pi m(\xi-x)/a]}{m}e^{-\pi m|\eta-y|/a} \\
&= -\frac{1}{4\pi}\ln\left[1 - 2e^{-\pi|\eta-y|/a}\cos\frac{\pi(\xi-x)}{a} + e^{-2\pi|\eta-y|/a}\right] \\
&= -\frac{1}{4\pi}\ln\left\{(1-e^{-\pi|\eta-y|/a})^2 + 2e^{-\pi|\eta-y|/a}\left[1-\cos\frac{\pi(\xi-x)}{a}\right]\right\} \\
&\approx -\frac{1}{4\pi}\ln\left[\frac{\pi^2(\eta-y)^2}{a^2} + \frac{\pi^2(\xi-x)^2}{a^2}\right] \\
&= -\frac{1}{4\pi}\ln\left[\pi^2\frac{(\xi-x)^2+(\eta-y)^2}{a^2}\right].
\end{aligned} \tag{6.2}$$

One thus can see that the specially constructed Green's function of rather complex form reduces to the classical logarithmic Green's function for unbounded space: $-(\ln r)/(2\pi)$, $r = [(\xi - x)^2 + (\eta - y)^2]^{1/2}$ when $r \to 0$.

Let contour l in BIE (4.6) consist of array of linear cracks l_n, $n = 1, \ldots, N_c$. Each crack is defined by its central point with Cartesian coordinates (c_n, d_n), by its length ζ_n, and by the angle of slope θ_n ($|\theta_n| \le \pi/2$) with respect to x-axis. If the n-th crack contains J_n grid nodes with the unique step $h = \zeta_n/J_n$, then the full set of nodes is a union of ones varying over all elementary cracks, as follows:

$$\begin{cases} X_i^{(n)} = c_n + [h(i - 0.5) - \zeta_n/2]\cos\theta_n, \\ Y_i^{(n)} = d_n + [h(i - 0.5) - \zeta_n/2]\sin\theta_n \end{cases} \quad (i = 1, \ldots, J_n; n = 1, \ldots, N_c). \tag{6.3}$$

Once again, the total number of grid nodes is equal to $J = \sum_{n=1}^{N_c} J_n$.

It should be noted that the grid nodes over any crack are distributed so that they are situated just at the half-way point between the end-points of a current elementary segment. Such an arrangement provides a symmetry so desired for any algorithm. In frames of such an approach, the integrals over small vicinity of the logarithmic singularity can be calculated explicitly. This calculation is founded on the following observation. If $(\xi, \eta) \to (X, Y)$ in (4.6), then both points (ξ, η) and (X, Y) lie on the same crack l_n, hence

$$\eta - Y = (\xi - X)\tan\theta, \quad dl = \frac{d\xi}{\cos\theta}. \tag{6.4}$$

Therefore, the sought integral over small neighborhood γ of the singular point, with the use of (6.2), is (assuming function $g(\xi, \eta)$ to be constant on the small elementary interval)

$$\begin{aligned} V &= \int_\gamma \Phi(\xi, \eta, X, Y)\,dl \approx -\frac{1}{4\pi}\int_\gamma \ln\left[\pi^2 \frac{(\xi - X)^2 + (\eta - Y)^2}{a^2}\right] dl \\ &= -\frac{1}{4\pi}\int_{X - h\cos\theta/2}^{X + h\cos\theta/2} \ln\left[\pi^2 \frac{(\xi - X)^2}{a^2\cos^2\theta}\right] \frac{d\xi}{\cos\theta} \\ &= -\frac{1}{\pi}\int_0^{h\cos\theta/2} \frac{\ln\xi - \ln(a\cos\theta/\pi)}{\cos\theta}\,d\xi \\ &= -\frac{1}{\pi}\left[\frac{\xi(\ln\xi - 1)}{\cos\theta}\bigg|_{\xi=0}^{\xi = h\cos\theta/2} - \frac{h}{2}\ln\left(\frac{a\cos\theta}{\pi}\right)\right] = \frac{h}{2\pi}\left(1 - \ln\frac{\pi h}{2a}\right). \end{aligned} \tag{6.5}$$

Note that this quantity is universal for all cracks from the cluster and for all grid nodes. It is meaningful that quantity V is free of any geometrical parameter of the current crack including slope angle θ.

Now, by changing the integral in the basic BIE (4.6) taken all over the cracks with the discretization as discussed above, the latter can be reduced to the following algebraic system:

$$\sum_{j=1}^{J} a_{ij} g_j = p_{0i}, \qquad i = 1, \ldots, J, \tag{6.6a}$$

with

$$\begin{aligned} &g_i = g(X_i, Y_i), \qquad a_{ii} = V, \qquad (X_j, Y_j) \in l, \qquad (X_i, Y_i) \in l, \\ &p_{0i} = p_0(X_i, Y_i) = \frac{2s_0}{a} \sum_{m=1}^{\infty} \sin\left(\frac{\pi m X_i}{a}\right) \sin\left(\frac{\pi m x_0}{a}\right) \frac{\sinh[q_m(b - Y_i)]}{\sinh(q_m b)}, \\ &\text{if } i \neq j: \qquad a_{ij} = \frac{h}{a} \sum_{m=1}^{\infty} \frac{\sin(\pi m X_j/a) \sin(\pi m X_i/a)}{q_m \sinh(q_m b)} \\ &\times \{\cosh[q_m(b - |Y_j - Y_i|)] - \cosh[q_m(b - Y_j - Y_i)]\}. \end{aligned} \tag{6.6b}$$

This system with the quadratic matrix $A = \{a_{ij}\}$ of dimension $J \times J$ is constructed so that the set of the ''inner'' discrete integration points $\{(\xi_j, \eta_j)\}$, over which the integration is being performed, coincides with the set of the ''outer'' nodes $\{(X_i, Y_i)\}$, which are used to provide the equality between the left- and the right-hand sides in (4.6). This is indeed the collocation technique, because $(\xi_j, \eta_j) = (X_j, Y_j)$, and so there is no need to differ the nodes (ξ_j, η_j) from (X_j, Y_j) in the discrete form of BIE.

Coming to the formulated reconstruction problem, let us estimate the total number of unknown parameters to be reconstructed. If the number of cracks is N_c, then for each of them one has 4 unknown parameters: c_n, d_n, ζ_n, θ_n, $(n = 1, \ldots, N_c)$. Therefore, the total number of unknown parameters is $4N_c$.

In order to find all these unknowns, we construct an objective functional, and reduce the reconstruction to an optimization problem for this functional. For this purpose let us represent system (6.6) in the operator form

$$\mathbf{A}g = p_0, \quad \mathbf{A} = \{a_{ij}\}, \quad g = \{g_i\}, \quad p_0 = \{p_{0i}\}, \quad (i, j = 1, \ldots, J), \tag{6.7}$$

whose solution can be expressed in terms of the inverse matrix, as follows:

$$g = \mathbf{A}^{-1} p_0, \qquad \Rightarrow \qquad g_i = (\mathbf{A}^{-1} p_0)_i. \tag{6.8}$$

Obviously, operator $\mathbf{A}^{-1}$ depends upon all $4N_c$ parameters: $\mathbf{A}^{-1} = \mathbf{A}^{-1}(c_n, d_n, \zeta_n, \theta_n)$.

Now, let us address the question: What is the measured information that can be used as input data for the reconstruction problem? We assume that a number of ultrasonic sensor probes can be placed uniformly over the boundary lines of the rectangular specimen, in order to register the amplitudes of its vibration at the chosen points (x_K, y_K), $K = 1, 2, \ldots, K^*$. Even a single sensor can be used for this aim if one puts it in turn on the same chosen points. Recall that we suppose these amplitudes to be given by respective boundary values of normal derivative of the acoustic pressure, function F_0 in (5.1). Now by substitution of (6.8) into (5.1), with the use of (5.2), one comes to the system of nonlinear equations for parameters c_n, d_n, ζ_n, θ_n written in the following discrete form:

$$\begin{aligned}
&\frac{h}{a}\sum_{j=1}^{J}[\mathbf{A}^{-1}(c_n, d_n, \zeta_n, \theta_n)p_0]_j \sum_{m=1}^{\infty}\frac{\sin(\pi m X_j/a)}{\sinh(q_m b)} \\
&\quad\times\left\langle \frac{\pi m}{a\, q_m}\cos\left(\frac{\pi m\, x_K}{a}\right)\{\cosh[q_m(b-|Y_j-y_K|)] \right.\\
&\quad -\cosh[q_m(b-Y_j-y_K)]\}n_x \\
&\quad +\sin\left(\frac{\pi m x_K}{a}\right)\{\sinh[q_m(b-|Y_j-y_K|)]\operatorname{sign}(Y_j-y_K) \\
&\quad \left.+\sinh[q_m(b-Y_j-y_K)]\}n_y\right\rangle \\
&\quad = -F_0(x_K, y_K), \qquad K = 1, \ldots, K^*, \qquad (x_K, y_K) \in L.
\end{aligned} \tag{6.9}$$

It is interesting to compare the number of unknown parameters and the number of equations. As indicated above, the first quantity is $4N_c$. Obviously, the second one is equal to the number of sensor positions, K^*. Subject to which quantity is greater among these two, system (6.9) may be underdetermined, overdetermined, or well determined. In every case, it is unclear how one can solve this system directly. Intuitively, one could suppose the more sensor measurement points the higher precision of the reconstruction. The method proposed here works well for any input data. It is thus irrelevant to which case from the three ones described above takes place indeed and what is the real number of the sensor points. Obviously, the number of the

sensor points may affect the precision of the reconstruction. However, the technique itself is universal with respect to this number.

The system of Eqs. (6.9) can be resolved by a minimization of the discrepancy functional:

$$
\begin{aligned}
&\min[\Omega(c_n,d_n,\zeta_n,\theta_n)],\quad \Omega(c_n,d_n,\zeta_n,\theta_n)\\
&=\left|\left|F_0(x_K,y_K)+\frac{h}{a}\sum_{j=1}^{J}[\mathbf{A}^{-1}(c_n,d_n,\zeta_n,\theta_n)p_0]_j\sum_{m=1}^{\infty}\frac{\sin(\pi mX_j/a)}{\sinh(q_mb)}\right.\right.\\
&\times\left\langle\frac{\pi m}{aq_m}\cos\left(\frac{\pi m\,x_K}{a}\right)\{\cosh[q_m(b-|Y_j-y_K|)]\right.\\
&-\cosh[q_m(b-Y_j-y_K)]\}n_x\sin\left(\frac{\pi mx_K}{a}\right)\{\sinh[q_m(b-|Y_j-y_K|)]\mathrm{sign}(Y_j-y_K)\\
&\left.\left.+\sinh\left[q_m(b-Y_j-y_K)]\right\}n_y\right\rangle\right|\Big|^2=\sum_{K=1}^{K^*}\Bigg\{F_0(x_K,y_K)\\
&+\frac{h}{a}\sum_{j=1}^{J}[\mathbf{A}^{-1}(c_n,d_n,\zeta_n,\theta_n)p_0]_j\sum_{m=1}^{\infty}\frac{\sin(\pi mX_j/a)}{\sinh(q_mb)}\\
&\times\left\langle\frac{\pi m}{a\,q_m}\cos\left(\frac{\pi m\,x_K}{a}\right)\{\cosh[q_m(b-|Y_j-y_K|)]\right.\\
&-\cosh[q_m(b-Y_j-y_K)]\}n_x\sin\left(\frac{\pi mx_K}{a}\right)\{\sinh[q_m(b-|Y_j-y_K|)]\mathrm{sign}(Y_j-y_K)\\
&\left.+\sinh\left[q_m(b-Y_j-y_K)]\right\}n_y\right\rangle\Bigg\}^2.
\end{aligned}
\tag{6.10}
$$

It should be noted that in the case of absolute precision in the input data the true geometry of the cracks' cluster returns zero minimum value to functional Ω. However, there arises the problem of uniqueness since we cannot prove that only true geometry of the cracks makes this functional trivial.

The minimization of functional (6.10) can be attained by any classical method of optimization [17,18]. However, the main restriction of regular iterative schemes is that they give a local minimum of respective functional only. Another difficulty is connected with a non-uniqueness of the solution, the question already discussed above but to be concerned again in a different aspect. Namely, it is not evident that a local minimum is at the same time the global minimum of the functional. In fact, it is well known that for nonlinear equations such values of local minima may be too far from the desired value $\Omega=0$.

For this reason, we used in our numerical experiments a version of the method of global random search contiguous to the one described in detail in [19]. This algorithm is developed to seek maxima, but it can be applied to minima too. It is constructed so that it moves both up-hill and downhill, and as the optimization process proceeds, it focuses on the most promising area. As a first step, it randomly chooses a trial point within the step of the user selected starting point. The function is evaluated at this trial point, and its value is compared to its value at the initial point. In a maximization problem, all uphill moves are accepted, and the algorithm continues from that trial point. Downhill moves may be accepted. It uses objective function F and the size of the downhill move in a probabilistic manner. The smaller F and the size of the downhill move are, the more likely that move will be accepted. The relationship between the initial value of F and the resulting step length is function dependent. This algorithm shows perfect convergence for many problems, also for our inverse problem, but unfortunately sometimes it arrives at a local extremum, instead of global one, in the cases when there are a lot of global minima of the objective function.

The algorithm applied is a slight modification of this idea. It possesses the two following specific features: 1) random sampling of values in the neighborhood of the points, for which the values of the functional are smaller, happens more frequently than in the neighborhood of worse points, and 2) the domains, in which random values of variables are chosen, are gradually contracted to the small neighborhoods of the points with smaller values of the functional. This technique demonstrates remarkable convergence for all considered examples.

Let us test the proposed method on the example of quadratic sample of the size $a=b=50$cm. If one applies ultrasonic probes with the cyclic frequency $f=100\,\text{kHz}$ and the average wave speed $3\,\text{km}/s$, then the wave length is $\lambda=3\cdot10^3/100\cdot10^5=0.03\,\text{m}=3\,\text{cm}$. For this combination of physical and geometric parameters, in spite of all series over parameter m converge as geometric progressions, a lot of initial terms correspond to the case when quantities q_m are not real but imaginary valued. For such m the hyperbolic functions transform to respective trigonometric ones, which do not decrease with m. This happens, with m increasing, until the expression under the root square in the definition of q_m, Eq. (3.3), becomes positive. Namely, this occurs when m precedes M for which $\pi M/a>k$, $\sim M>ak/\pi=2a/\lambda$. In the considered examples with $\lambda=3\,\text{cm}$ and $a=50\,\text{cm}$, one can estimate that first 33 terms in all series are not exponentially decaying.

It should also be noted that the intersection of cracks is permissable in the structure, since the formulated BIE is valid in this case too.

For all examples listed below, the input data for the reconstruction is taken from the solution of respective direct problem. In our simulation, we always used $K_s=20$ points of measurements, uniformly distributed on each side of the quadratic domain. These 20 points are placed at the central position of 20 equal subintervals of the respective side, so that to guarantee that

all sensors are located with a minimal distance from the corners of the specimen. It is obvious that the total number of sensor positions is $K^* = 4K_s = 80$, again uniformly distributed over full boundary contour of the rectangular domain. For all examples demonstrated below we used the position for the acoustic source on the bottom of the sample to be $x_0 = a/2$, i.e., at the center of its lower face. Besides, the maximum possible number of cracks in the cluster is taken $N^* = 5$.

Let us estimate the efficiency of the proposed algorithm, in the case related to typical examples considered below and applied with 500 iterations in the described stochastic search, with 30 trials on each iteration step, for every of N^* combinations of the number of cracks. The algorithm thus uses $30 \times 500 \times 5 = 75.000$ trials of the objective functional Ω that takes near one hour of calculations when implemented on PC with AMD Athlon Core2 processor of 6.0 HGz CPU clock (recall that each trial requires solution of the basic BIE system). If anyone would apply direct search by an enumerative technique, then one would calculate functional Ω depending upon desired scale in the precision of all geometric parameters of the cracks. Let in the poorest case one take 50 values for a and b (with the scale 1 cm). Let then the maximum crack length be 18 cm and the minimum one 3 cm (coinciding with the wave length), with the same scale 1 cm and at least 10 possible values for the slope angle θ. Then for each crack, one should apply $50 \times 50 \times 15 \times 10 = 375.000$ trials. In total, one should apply $(375.000)^{N^*}$ trials, where N^* is the maximum possible number of cracks. The reader can easily understand that the calculation time for such ''direct'' numerical experiments exceeds the capabilities of any existing computer.

It is obvious that the proposed algorithm, in the particular case when the admitted maximum number of cracks is $N^* = 1$, can be used for any single crack reconstruction. An example of this sort is demonstrated in Table 1. All sizes are given in cm. As can be seen from the table, in the case of single crack the reconstruction seems to be perfect.

Some examples on the reconstruction of multiple arrays of cracks are presented in Tables 2 and 3.

For multiple cracks array the algorithm works so that this selects the most likely geometry, sequentially for $N_c = 1, 2, 3, 4, 5$ number of cracks (recall that $N^* = 5$ for all considered examples). Then the algorithm makes a choice on the best value of functional Ω, among these 5 geometries, to come to the true solution.

TABLE 1 Results of the Reconstruction, Single Crack, 500 and 1000 Iterations

c	d	ζ	θ	Type of result	Ω
14.968	34.935	9.797	1.047	reconstructed, 500 iter.	$0.776 \cdot 10^{-1}$
15.009	35.019	10.044	1.047	reconstructed, 1000 iter.	$0.444 \cdot 10^{-2}$
15	35	10	$\pi/3 = 1.047$	exact	0

TABLE 2 Results of the Reconstruction, Three Cracks, 500 and 1000 Iterations

Crack	c	d	ζ	θ	Type of result	Ω
1st	14.599	35.143	9.102	0.933	reconstructed,	0.207
2nd	26.207	25.323	4.574	−0.142	500 iter.	
3rd	32.373	29.205	9.261	−0.662		
1st	15.630	34.996	10.345	1.177	reconstructed,	$0.834 \cdot 10^{-1}$
2nd	23.953	24.868	5.077	0.033	1000 iter.	
3rd	35.689	29.481	9.893	−0.681		
1st	15	35	10	$\pi/3 = 1.047$	exact	0
2nd	25	25	6	0		
3rd	35	30	10	$-\pi/4 = -0.785$		

From the presented results of the numerical simulation one can extract the following conclusions:

1. Typically, functional Ω, if one applies it with a randomly chosen set of four parameters c, d, ζ, θ, varies from the characteristic value $10^2 - 10^3$ (single crack) up to characteristic value $10^5 - 10^7$ (five cracks). This information is helpful when evaluating precision of the reconstruction reflected in Tables 1–3. One thus can see that the absolute attained minimal value of Ω for multiple cracks is not so poor when compared to the case of single crack.
2. In the reconstruction of single crack the behavior of the convergence is typically monotonic, in the sense that with the number of the iteration step increasing all four parameters become closer to their exact values,

TABLE 3 Results of the Reconstruction, Five Cracks, 500 and 1000 Iterations

Crack	c	d	ζ	θ	Type of result	Ω
1st	14.663	37.308	9.710	1.167	reconstructed,	$0.196 \cdot 10^{1}$
2nd	25.986	25.754	4.147	−0.207	500 iter.	
3rd	34.861	27.318	12.076	−0.841		
4th	28.195	9.483	14.404	0.540		
5th	37.904	37.055	7.713	1.524		
1st	15.279	34.304	10.677	1.055	reconstructed,	0.708
2nd	23.849	25.831	5.967	0.189	1000 iter.	
3rd	35.874	29.802	10.206	−0.837		
4th	31.112	13.034	12.939	0.546		
5th	37.955	37.144	8.156	1.519		
1st	15	35	10	$\pi/3 = 1.047$	exact	0
2nd	25	25	6	0		
3rd	35	30	10	$-\pi/4 = -0.785$		
4th	30	12	13	$\pi/6 = 0.524$		
5th	38	38	8	$\pi/2 = 1.571$		

and so is the value of functional Ω. Note that respective exact values in our test examples are known a priori since they are constructed from direct problems.

3. If we construct the input data from respective direct problem without any random perturbation, which is used sometimes in simulation of inverse problems, then it is obvious that the value of the discrepancy functional is zero for the exact solution. The influence of the error in the input data on precision of the reconstruction will be studied in a next paper of the present authors. However, here we would like to note that for exact input data the behavior of Ω versus number of iteration steps is typically monotonic, even in the case of multiple cracks.
4. The convergence of the reconstructed parameters versus iteration number is typically not monotonic. This means that after more iteration steps some parameters may approach closer to their exact values; however, some other parameters sometimes may be slightly more distant from respective exact values. This is quite natural in multidimensional optimization, since a smaller value of the discrepancy functional does not always mean closer values for all variables to their exact quantities.

ACKNOWLEDGEMENTS

The present work has been supported in part by Italian Ministry of University (M.U.R.S.T.) through its national and local projects. The work is also supported by the Russian Federal Targeted Programme ''Scientific and Scientific- Educational Personnel of Innovative Russia'' for 2009–2013, Project 02.740.11.5024.

REFERENCES

1. J. Daniels. *Surface Penetrating Radar*. Inst. Electr. Eng., London (1996).
2. L. Binda, G. Lenzi, and A. Saisi. *J. NDT and E Intern.* **31**:411–419 (1998).
3. C. Maierhofer, and S. Leipold. *J. NDT and E Intern.* **34**:139–147 (2001).
4. J. Krautkrämer and H. Krautkrämer. *Ultrasonic Testing of Materials*. Springer-Verlag, Berlin (1983).
5. A. Friedman and M. Vogelius. *Indiana Univ. Math. J.* **38**:527–556 (1989).
6. G. Alessandrini, E. Beretta, and S. Vessella. *SIAM J. Math. Anal.* **27**:361–375 (1996).
7. A. B. Abda et al. *Inverse Probl.* **18**:1057–1077 (2002).
8. D. Colton and R. Kress. *Integral Equation Methods in Scattering Theory*. John Wiley, New York (1983).
9. D. Colton and R. Kress. *Inverse Acoustic and Electromagnetic Scattering Theory*. Springer-Verlag, Berlin (1992).
10. R. Potthast. *Point Sources and Multipoles in Inverse Scattering Theory*. Chapman & Hall, London (2001).
11. A. N. Tikhonov and V. Y. Arsenin. *Solutions of Ill-posed Problems*. Winston, Washington (1977).
12. M. Bonnet. *Boundary Integral Equations Methods for Solids and Fluids*. John Wiley, New York (1999).
13. R. Courant and D. Hilbert. *Methods of Mathematical Physics, vol.1*. Interscience Publ., New York (1953).

14. K. D. Cole and D. H. Y. Yen. *Green's functions, temperature and heat flux in the rectangle, Int. J. Heat Mass Transfer* **44**:3883–3894 (2001).
15. B. B. Guzina, S. N. Fata, and M. Bonnet. *Electronic Journal of Boundary Elements* **2**:223–230 (2002).
16. I. S. Gradshteyn and I. M. Ryzhik. *Table of Integrals, Series, and Products* (5th ed.). Academic Press, New York (1994).
17. L. V. Kantorovich and G. P. Akilov. *Functional Analysis*. Pergamon Press, Oxford (1982).
18. P. E. Gill, W. Murray, and M. H. Wright. *Practical Optimization*. Academic Press, London (1981).
19. M. Corana et al. *ACM Trans. Math. Software* **13**:262–280 (1987).